POTENTIAL INHIBITORS OF COPD-RELEVANT SERINE PROTEASES BASED ON THE N-AMINO-4-IMIDAZOLIDINONE SCAFFOLD

A Thesis by

Guijia He

Bachelor of Science Sichuan University, 1998

Submitted to the Department of Chemistry
and the faculty of the Graduate School of
Wichita State University
in partial fulfillment of
the requirement for the degree of
Master of Science

December 2009

POTENTIAL INHIBITORS OF COPD-RELEVANT SERINE PROTEASES BASED ON THE N-AMINO-4-IMIDAZOLIDINONE SCAFFOLD

The following faculty members have examined the final copy or this thesis for form and content, and recommend that it be accepted in partial fulfillment of the requirement for the degree of Master of Science with a major in chemistry.

_____
William C. Groutas, Committee Chair

_____
James G. Bann, Committee Member

_____
David M. Eichhorn, Committee Member

_____
Michael Van Stipdonk, Committee Member

_____
Lop-Hing Ho, Committee Member

ACKNOWLEDGMENTS

I would like to express my heartfelt gratitude to my advisor, Dr. Groutas for his tremendous guidance and support in my graduate study and research. He has given me so much kindness, and led me to ascend to a higher level in the field of organic and medicinal chemistry. I thank him so much for giving me this opportunity to have such wonderful memory of working in his group and being a graduate student at Wichita State University.

I am also greatly indebted to my committee members, Dr. Bann, Dr. Eichhorn, Dr. Van Stipdonk and Dr. Ho, for their instruction and helpful advice.

Furthermore, I want to thank all of our research group members, Liuqing Wei, Qingliang Yang, Dengfeng Dou, Sridhar Aravapalli, Sivakoteswararao Mandadapu, and Kok Chuan Tiew, for their help on my research; and Dr. Kevin R. Alliston, and Yi Li, for their help on my biochemical study.

Especially, I would like to express my heartfelt gratitude to my husband, Dengfeng Dou, for his great help in both my academic and our family life. And I thank my cute little boy, Qi Dou, for the joys he gives me. I want to thank my parents. I would never have gone this far without their understanding and strong support.

Finally, I owe my sincere gratitude to my friends who give me their help and time in my English and graduate studies.

ABSTRACT

Human neutrophil elastase (HNE) and proteinase 3 (PR3) are serine proteases which play a crucial role in the pathogenesis of chronic obstructive pulmonary disease (COPD), a multifactorial disorder associated with an imbalance between the levels of COPD-relevant proteases and their physiological protein inhibitors. The N-amino-4-imidazolidinone scaffold was used in the design and synthesis of potential inhibitors of HNE and PR3. The results show that this is a promising avenue of investigation for the development of reversible competitive inhibitors with good selectivity toward HNE and PR3. Molecular docking simulations are supportive of the validity of this approach.

TABLE OF CONTENTS

TABLE OF CONTENTS (continued)

LIST OF FIGURES

LIST OF FIGURES (continued)

LIST OF TABLES

LIST OF SCHEMES

LIST OF ABBREVIATIONS

Abu	2-Aminobutyric Acid
Arg	Arginine
Ala	Alanine
Asp	Aspartic acid
Boc	*tert*-Butyloxycarbonyl
Cat G	Cathepsin G
COPD	Chronic Obstructive Pulmonary Disease
Cys	Cysteine
DFP	Diisopropylfluorophosphate
DMSO	Dimethyl Sulfoxide
E	Enzyme
EI	Enzyme-inhibitor Complex
ES	Enzyme-substrate Complex
Gly	Glycine
HEPES	4-(2-Hydroxyethyl)-1-piperazine -ethanesulfonic Acid
His	Histidine
HNE	Human neutrophil elastase
I	Inhibitor
[I]	Inhibitor Concentration
IBCF	Isobutyl Chloroformate
Ile	Isoleucine
K_M	Michaelis-Menten Constant
Leu	Leucine
Lys	Lysine
MMP-12	Macrophage Metalloelastase 12
NMM	N-methylmorpholine
Nva	Norvaline
P	Product
Pd-C	Palladium on Carbon
Phe	Phenylalanine
Pro	Proline
PR3	Proteinase 3
RT.	Room temperature
S	Substrate
[S]	Substrate Concentration
SBzl	Thiobenzyl
Ser	Serine
THF	Tetrahydrofuran
TS	Transition state
$1/v$	Reciprocal of Velocity
Val	Valine
Z	Carbobenzyloxy

CHAPTER 1

INTRODUCTION

1.1 What is COPD?

COPD (chronic obstructive pulmonary disease) is a progressive disease that is associated with an abnormal inflammatory response of the lungs to noxious particles or gases and is a major cause of disability [1]. COPD is the fourth leading cause of death in the United States and worldwide by 2020 it is predicted to be the third most frequent cause of death [2, 3]. COPD is one of the few chronic diseases that have shown an increase in mortality in recent years [3]. Cigarette smoking is the primary cause of COPD [4, 5], although it has also been linked to other additional factors such as genetic susceptibility, air pollution and other airborne irritants [6, 7].

There are three main respiratory pathologies in COPD: emphysema, respiratory bronchiolitis and chronic bronchitis [1]. In these conditions, the disruption of the alveolar walls and elastin leads to a decrease in the elastic recoil of the lungs, limiting the ability of the alveoli to passively shrink and to exhale. The bronchial tubes and alveoli are damaged and lose their elastic quality, the walls between many of the alveoli are destroyed or the walls of the bronchial

tubes become thick and inflamed. Although COPD is primarily a disease of the lungs, it is now established as a disease associated with systemic characteristics [3].

COPD is an irreversible condition and cannot be cured now. Current treatment can only slow its progression. Although the pathogenesis of COPD is poorly understood [8], the disorder is characterized by increased numbers of alveolar macrophages, neutrophils and cytotoxic T lymphocytes [9, 10], increased elastolysis by an array of proteases, oxidative stress, apoptosis [11, 12], and the release of multiple inflammatory mediators [13]. Elucidation of the biochemical and molecular mechanisms related to the pathophysiology of this multifacatorial disorder may lead to the emergence of effective therapeutics.

1.2 Enzymes Involved in COPD

A number of enzymes believed to be relevant with COPD are serine proteases, including human neutrophil elastase (HNE) [14], proteinase 3 (PR3) [15], cathepsin G (Cat G) [14] and matrix metalloproteinase (MMP) [16]. In response to toxins in the smoke, macrophages and other phagocytic cells release COPD-relevant enzymes that degrade the extracellular matrix. The enzymes related to the research described in this thesis are HNE and PR3.

1.2.1 An Overview of Proteases

Proteases are a group of enzymes that hydrolyze peptide bonds in proteins. They exist widely among animals, plants and microorganisms. Proteases are important in many physiological processes, including digestion due to this catalytic function by breaking down the polypeptide bonds in the protein food to furnish amino acids that are crucial for normal functioning.

Proteases are currently classified into six groups based on catalytic mechanism: serine proteases, cysteine proteases, aspartic proteases, matrix metalloproteases, threonine proteases and glutamic acid proteases.

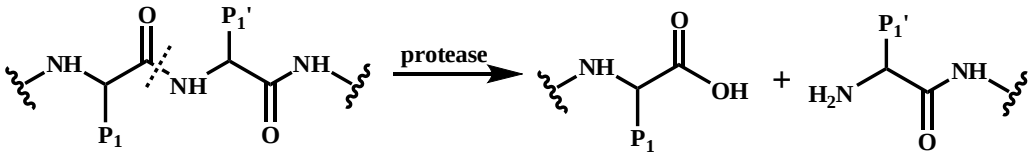

Figure 1.1 The hydrolysis reaction catalyzed by proteases

1.2.2 Nomenclature

Hydrolysis of a peptide bond by a protease involves binding of a peptide or protein substrate to the active site of the protease. The active site of a protease contains catalytic and

binding sites. It consists of an array of pockets or clefts with different shapes surrounded by side chains at the surface of the enzyme that are responsible for substrate specificity. The peptide bond of a substrate which is hydrolyzed is called the scissile bond. According to the Schechter and Berger nomenclature [17] for the description of protease subsites, the enzyme subsites of the active site are called S (for subsites) and the substrate amino acid residues are called P (for peptide) [18]. The enzyme subsites are labeled as Sn, ……, S2, S1, S1', S2', ……, Sn' (S1-S1' is the scissile bond) from amino- to carboxy-terminal, and the corresponding substrate residues are labeled as Pn, ……, P2, P1, P1', P2', ……, Pn' (illustrated in Figure 1.2 below).

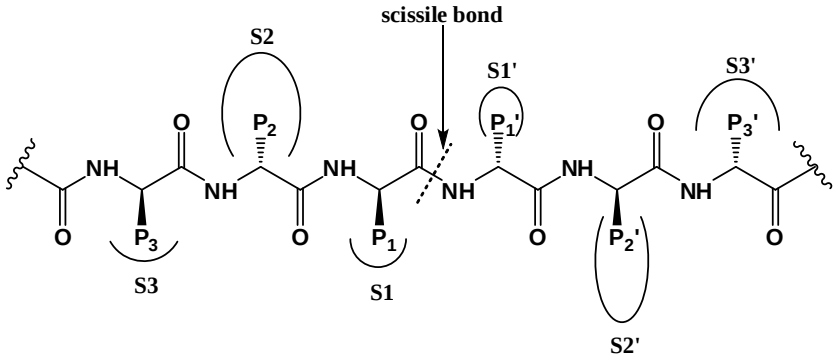

Figure 1.2 Schechter and Berger nomenclature for the description of protease subsites and amino acid residues of substrate

1.2.3 Enzyme-substrate Interactions

A substrate binds to the active site of an enzyme by non-covalent forces before the enzyme conducts its catalytic reaction (shown in Figure 1.3). Proximity effects between enzyme

and substrate are a major factor in enzyme catalysis. The interactions between enzyme and substrate include hydrogen bonds, dipole-dipole interactions, ion-ion interactions, hydrophobic interactions, cation-π interactions, etc. An enzyme will typically utilize multiple types of catalysis in performing its function.

Hydrogen bonds are the most common non-covalent forces in enzyme-substrate complexes. This kind of attractive interaction can be easily found between hydrogen atoms and electronegative atoms (oxygen, nitrogen) in the residues of substrates and active site of enzymes. Dipole-dipole interactions occur when enzymes or substrates contain atoms that are not electronegative enough, such as chlorine. There are several amino acids that have acidic or basic residues that generate anions or cations when deprotonated or protonated at different pH value, forming ion-ion interactions between each other. Hydrophobic interactions usually exist between enzyme and substrate which have residues like phenylalanine, alanine, leucine, etc. Amino acid side chains of tryptophan, tyrosine or phenylalanine are capable of engaging positive charged amino acid side chains, referred to as cation-π interactions.

$$E + S \underset{k_M}{\overset{k_1}{\rightleftharpoons}} ES \xrightarrow{k_{cat}} E + P$$

Figure 1.3 Michaelis-Menten model of enzyme kinetics

1.3 Mechanism and Substrate Specificity

1.3.1 Catalytic Mechanism of Serine Protease

An enzyme that hydrolyzes the peptide bond of a substrate by utilizing a serine residue located in its active site is referred to as a serine protease. Some of the serine proteases stored in the azurophilic granules of neutrophils, including HNE, PR3 and Cat G [19] play important roles in defending against bacterial and fungal infections in COPD [20].

Catalysis by serine proteases is accomplished by a catalytic triad which includes a serine, a histidine and an aspartic acid residue located in the active site. The catalytic mechanism of serine protease is shown in Figure 1.4. The catalytic triad is arranged in such a manner that the aspartic acid residue keeps the histidine ring in a fixed direction by hydrogen binding to facilitate the hydrogen bond between histidine and the serine residue. Following substrate binding, Ser195 attacks the carbonyl of the amide bond to form a tetrahedral oxyanion intermediate, which is stabilized by hydrogen bonds with the backbone of the enzyme (Figure 1.4 b), hence reducing the activation energy for the overall step [21]. The amide bond of the substrate cleaves after accepting a proton from the histidine to NHR' group. In the presence of a water molecule, the inactive acyl enzyme undergoes a neucleophilic substitution reaction (Figure 1.4 c). Protonation of the departing oxygen in the serine residue by His57 gives an active serine residue and leads to

the formation of a carboxylic acid product (Figure 1.4 e). The Asp102 is crucial to the catalysis of serine proteases by stabilizing the imidazolium cation of His57.

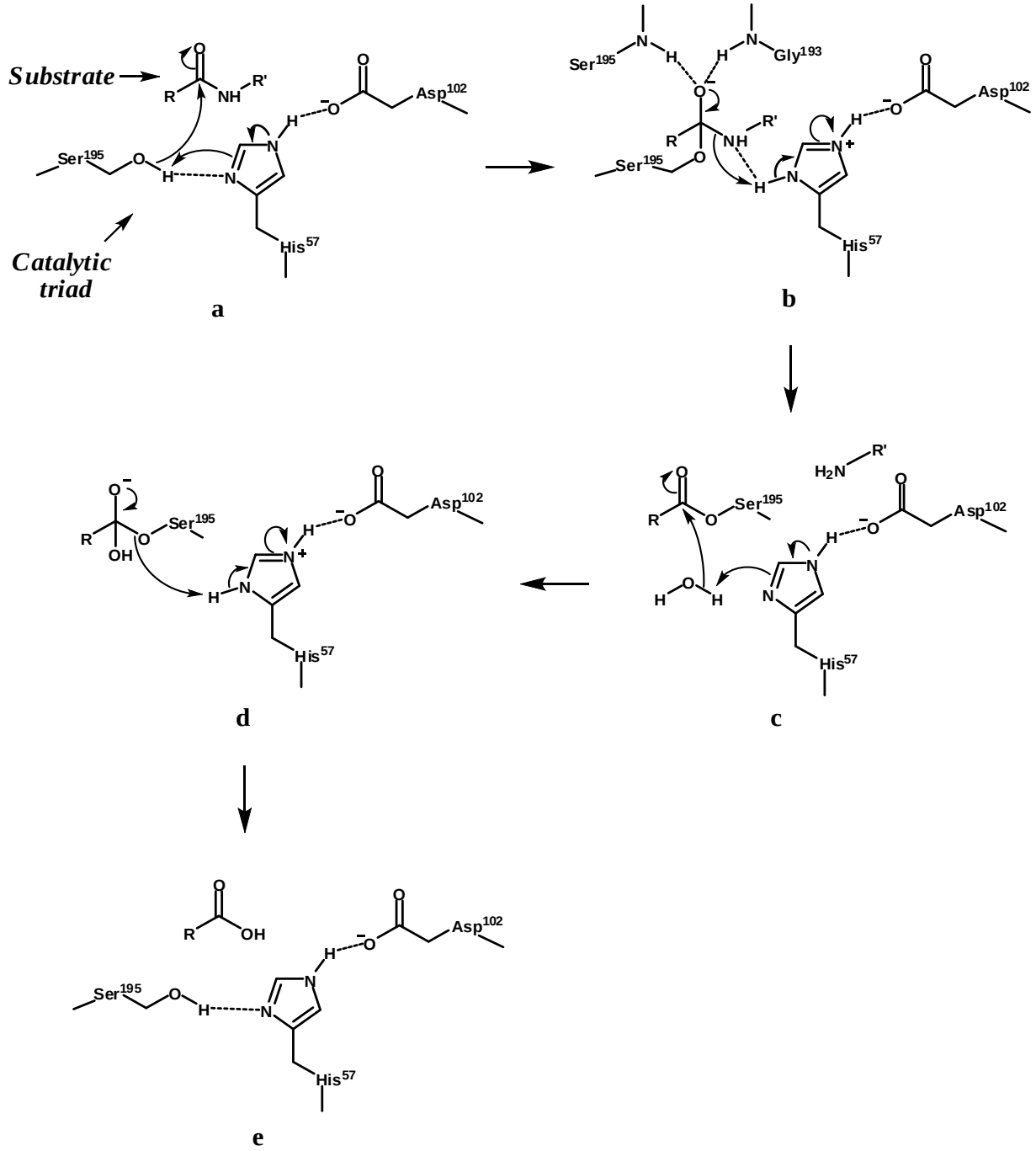

Figure 1.4 Catalytic mechanisms of serine proteases

1.3.2 Substrate Specificity

Substrate specificity refers to the characteristic feature of enzyme activity in relation to the kind of substrate with which the enzyme interacts. The lock and key model, first postulated by Emil Fischer in 1894, is a way of describing the interaction of a substrate and the active site of an enzyme (Figure 1.5A). This model assumed that enzyme and substrate are rigid and have exact complimentary shapes that fit each other. However, the bonds in enzymes are flexible. Enzymes can be induced to fit a substrate under the influence of different interactions between their side chains and the amino acid residues of a substrate (Figure 1.5B) [22].

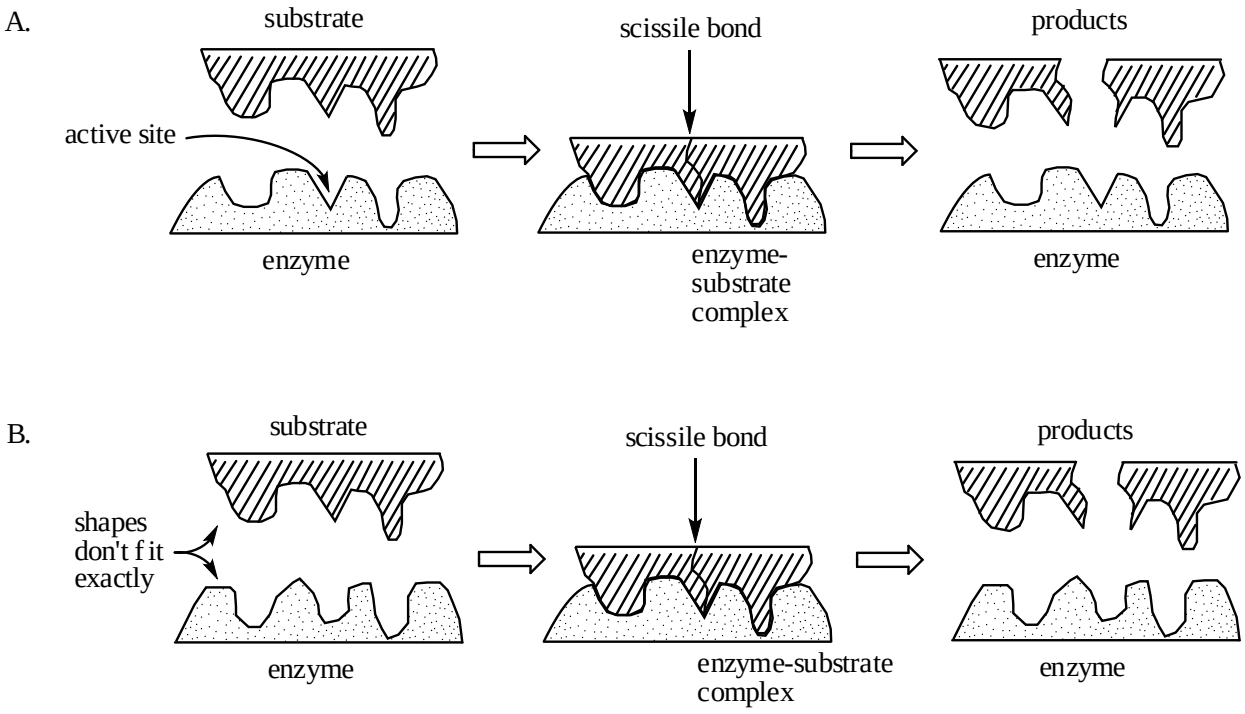

Figure 1.5 Binding models of substrates with enzymes. A. Lock and key model of enzyme – substrate binding; B. Induced-fit theory of enzyme – substrate binding

The catalytic efficiency of an enzyme is expressed by k_{cat}/K_M ($M^{-1}\cdot s^{-1}$) (see Figure 1.3). The bigger the k_{cat}/K_M is, the more efficient an enzyme is [23]. Substrate specificity is a crucial element used in mapping the active site of enzymes.

The two chymotrypsin-like serine proteases, HNE and PR3, have similar primary amino acid sequences (PR3 has 57% identity comparing to HNE). The substrate specificities of HNE and PR3 are given in Table 1.1

TABLE 1.1

COMPARISON OF THE SUBSTRATE SPECIFICITIES OF HNE AND PR3

	S4	S3	S2	S1	S1’	S2’	S3’
HNE	Ala	Val	Pro	Val	(Hydrophobic)		
PR3	Ala	Ala	Pro	Abu	Lys	Gly	Asp

1.3.2.1 Substrate Specificity of Human Neutrophil Elastase

Human neutrophil elastase (HNE: EC 3.4.21.37) has 218 amino acid residues with two sites of N-glycosylation, and was first isolated from the azurophilic granules of leukemia myeloid cells [24]. The X-ray crystal structure of the HNE-TOMI complex [25] shows the active site residues located in a cleft between two β-barrels. The presence of Val190, Phe192, Ala213,

Val216, Phe228 and the disulfide bridge Cys191-Cys220 makes the S1 pocket of HNE hemispherical and hydrophobic [26]. The S2 subsite of HNE, lined by Phe215, Leu99 and His57, explains the preference for medium-size, hydrophobic side chains. It has been demonstrated that the S1' subsite of HNE is relatively hydrophobic and lined by Cys42-Cys58 and Phe41 [27].

1.3.2.2 Substrate Specificity of Proteinase 3

Proteinase 3 (PR3: EC 3.4.21.76) consists of 221 amino acid residues (Mr 29 kDa) and is found in azurophilic granules of polyphonuclear neutrophils [28]. The S1-S4 subsites of PR3 are similar to those of HNE with a preference for small hydrophobic residues. The S1 pocket of PR3 is hemispheric but smaller than that of HNE due to the replacement of Val190 by Ile190. The substitution of Leu (HNE) to Lys (PR3) at position 99 leads to a deep polar pocket of increased polarity that prefers a negatively charged P2 in PR3. It has also been demonstrated that subsites S2, S1', and S2' are the main determinants of PR3 specificity [29, 30]. Asp61, located in vicinity of S1'-S3' in PR3, makes the pockets smaller and more polar than those of HNE. A preference of a negatively charged and more polar side-chain at P2' in substrate would improve its interaction with the S2' subsite of PR3 due to the presence of Arg143 and Pro151 instead of Leu143 and Ile151 in HNE [31]. It may be deduced that a consensus sequence for PR3 substrates

may extend from P2 to P3' including negative, small hydrophobic, positive, negative and positive residues respectively, which is not recognized by HNE [29, 30].

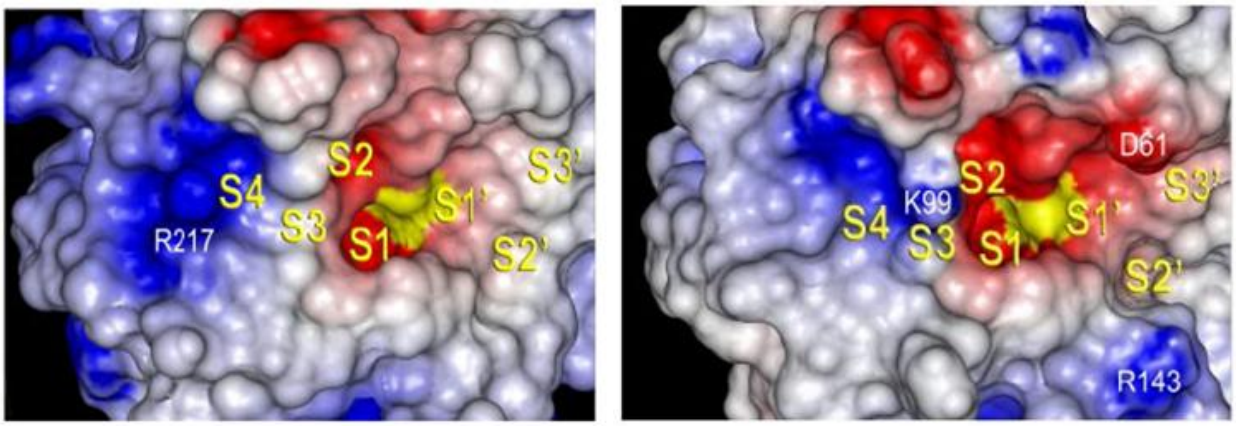

Elastase Proteinase 3

Figure 1.6 The crystal structures of HNE and PR3

1.4 Inhibitors

Molecules that bind to enzymes and decrease their activity are called inhibitors. The binding of an inhibitor with an enzyme prevents a substrate from occupying the active site, thus hinders its enzymatic catalysis. Some enzyme inhibitors that exist in the human body are involved in the regulation of metabolism. Many drugs function as enzyme inhibitors because blocking of enzyme activity can regulate metabolic imbalances or kill pathogens. The discovery of drugs that inhibit aberrant enzyme activity is an ongoing active area in biochemistry and pharmacology.

Like substrates, an inhibitor binds to enzyme, inhibiting its enzymatic activity (shown in Figure 1.7). Inhibitors bind to enzymes in an irreversible or reversible fashion. Thus, inhibitors are classified into irreversible and reversible inhibitors.

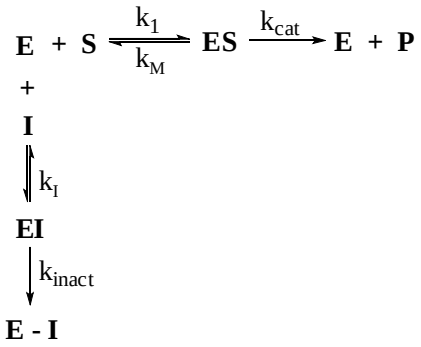

Figure 1.7 Binding model of irreversible inhibitor with enzyme competing with substrate

1.4.1 Irreversible Inhibitors

Irreversible inhibitors bind to the active site of enzymes forming non-covalent complexes (EI), then react with an active site group to form covalent bonds (E–I) [21]. Enzymes are inactivated permanently due to their active sites being irreversibly blocked by such inhibitors (Figure 1.7). The inactivation of an enzyme by an irreversible inhibitor is time-dependent (Figure 1.8).

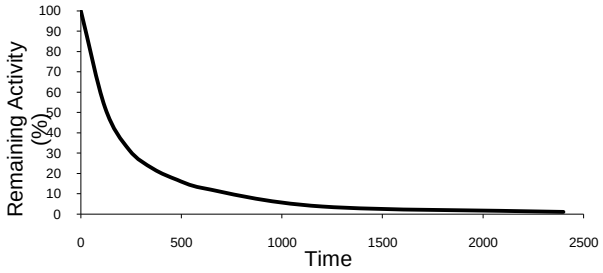

Figure 1.8 Remaining activity versus time plot illustrating time-dependent inactivation of enzyme by an irreversible inhibitor

There are two main classes of irreversible inhibitors: affinity labeling inhibitors and mechanism-based inhibitors. An affinity labeling inhibitor has a highly reactive group as part of its structure that reacts with a critical catalytic residue. Because of its high reactivity, an affinity labeling inhibitor usually lacks selectivity and has high toxicity. This kind of inhibitor includes alkylating agents, acylating agents, phosphorylating agents, carbamoylating agents, isocyanates or epoxides.

Mechanism-based inhibitors are molecules of low chemical reactivity that bind to the active site of an enzyme, and are converted into a highly reactive group ($E\text{-}I^{*}$) using the catalytic machinery of an enzyme. They subsequently react with an active site residue leading to irreversible inactivation of the enzyme ($E\text{-}I^{**}$) (Figure 1.9).

$$E + I \rightleftharpoons EI \longrightarrow E - I^{*} \longrightarrow E - I^{**}$$

Figure 1.9 Inactivation of an enzyme by a mechanism-based inhibitor

The potency of covalent inhibitors is expressed as $k_{obs}/[I]$ $M^{-1}s^{-1}$ or k_{inact}/K_I $M^{-1}s^{-1}$. k_{inact} is the rate constant of covalent reaction of enzyme-inhibitor complex. K_I is the dissociation constant of complex EI. A larger k_{inact}/K_I reflects a greater potency of the formation of covalent bond between enzyme and inhibitor, and less tendency of dissociation of enzyme-inhibitor complex.

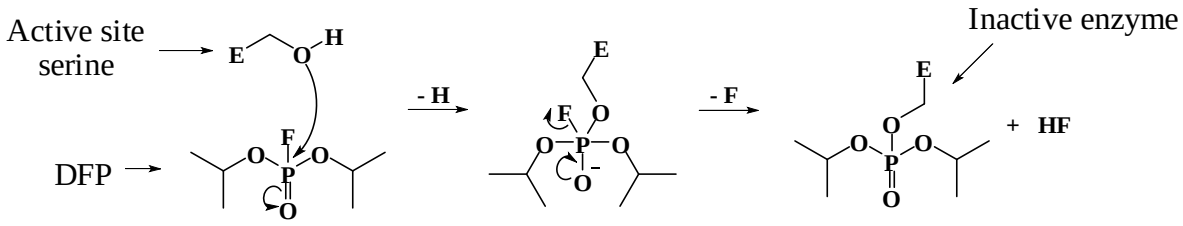

Figure 1.10 Irreversible inhibition of a serine protease by diisopropylfluorophosphate

1.4.2 Reversible Inhibitors

Reversible inhibitors do not form covalent bonds with enzymes. Instead, recognition elements incorporated in the inhibitor allow it to bind to the active site, preventing the approach of a substrate to the enzyme. Reversible inhibitors are usually more selective than irreversible inhibitors by virtue of their lower reactivity. There are several ways that a reversible inhibitor can block the active site of an enzyme. Thus, they are classified into classical reversible inhibitors, transition state inhibitors, slow binding inhibitors, and tight binding inhibitors.

1.4.2.1 Competitive Inhibitors

Competitive inhibitors, noncompetitive inhibitors, and uncompetitive inhibitors are three main classes of classical reversible inhibitors. Competitive inhibitors are compounds that have similar geometry as substrates, and bind to enzymes without further reaction (Figure 1.11). This kind of inhibitor competes with substrate in occupying the active site of an enzyme.

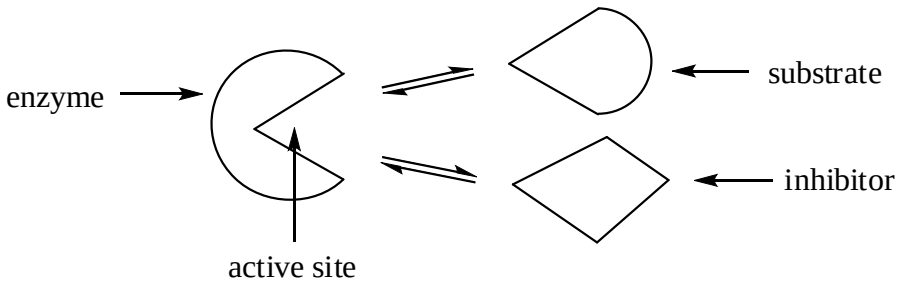

Figure 1.11 A competitive inhibitor competing with substrate towards an enzyme

Dixon plots (Figure 1.12) are used to establish whether an inhibitor is reversible competitive or noncompetitive. The reciprocal of velocity of the catalytic reaction versus inhibitor concentration is plotted under two different substrate concentrations. If the lines intersect behind the 1/v axis and above the [I] axis, the inhibitor is a competitive inhibitor. If the lines intersect at the [I] axis and behind the 1/v axis, it is a noncompetitive inhibitor. K_I is an For a competitive inhibitor, K_I is an index of the affinity of an inhibitor for an enzyme. The smaller the K_I is, the higher affinity an inhibitor has for an enzyme.

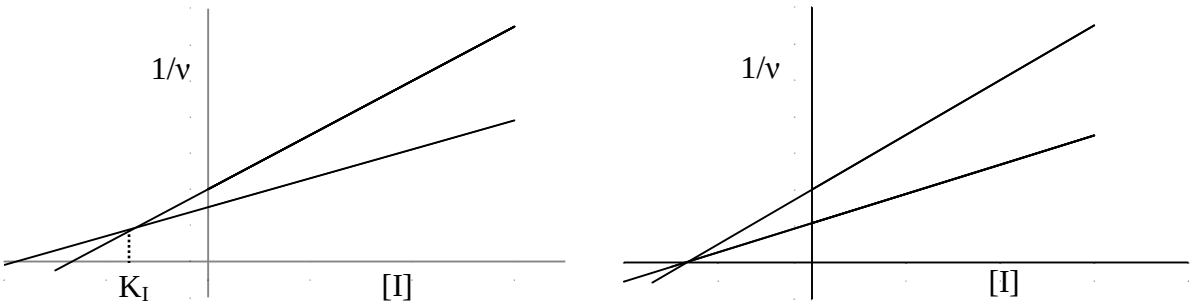

Figure 1.12 Dixon plots for a competitive and a noncompetitive inhibitor

1.4.2.2 Transition State Inhibitors

Another important type of reversible inhibitor is transition state inhibitor. The structure of a transition state inhibitor resembles that of the transition state of the reaction catalyzed by the enzyme. Enzymes bind transition states more tightly than ground states [32]. As shown in Figure 1.13A, enzymes bind with substrates more tightly in the geometry of the transition states. This is known as "transition-state stabilization" [33]. A transition state analog designed to mimic the geometry of the transition state of an enzymatic reaction makes a transition state inhibitor (Figure 1.13B). Examples of transition state inhibitors include α-keto esters, α-keto amides, boronic acids, trifluoromethyl ketones and others.

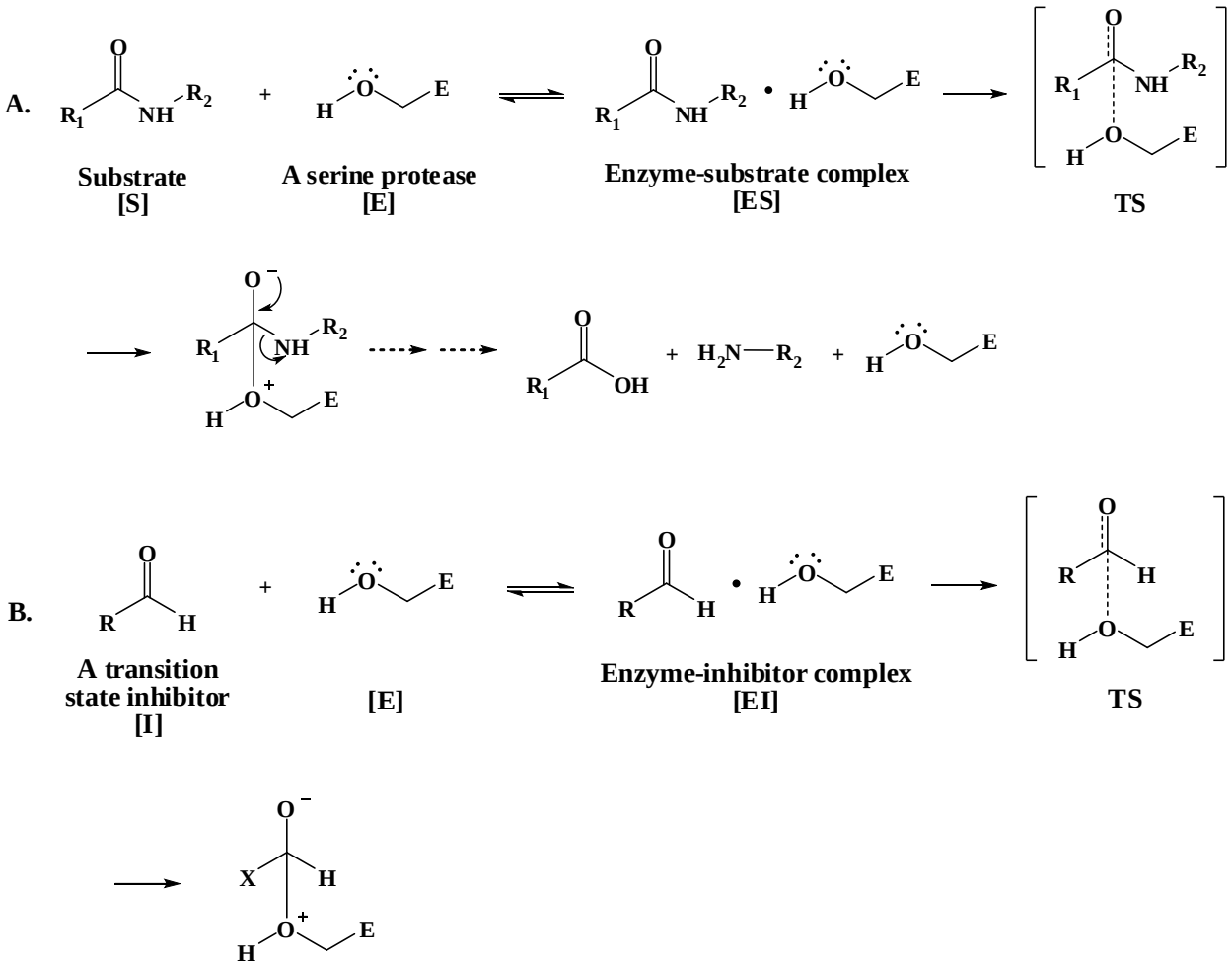

Figure 1.13 An enzyme binds the transition state of the reaction it catalyzes more tightly than the reactant: A. A serine protease forms with a substrate, and then hydrolyzes it; B. A serine protease binds a similar transition state with an inhibitor.

CHAPTER 2

DESIGN RATIONALE & RESEARCH GOALS

2.1 Inhibitor Design Rationale

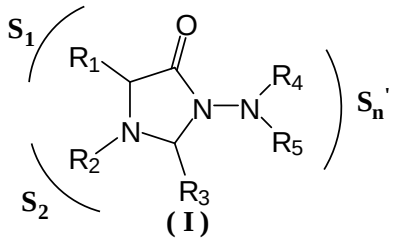

Figure 2.1 General structure of designed scaffold (I)

The crystal structure of the HNE-TOMI [25] complex was utilized in designing scaffold (I). The design is briefly described below: (a) recent studies in our laboratory have demonstrated that inhibitors based on scaffold (II, Figure 2.2) are highly efficient mechanism-based irreversible inhibitors of serine proteases [34]; (b) derivatives of 4-imidazolidinone (III) designed from prototype (II) have been found to be potent competitive inhibitors of HNE [35]. Thus, the replacement of sulfonyl to methylene group in the heterocyclic scaffold makes possible the conversion of irreversible inhibitors to reversible competitive inhibitors (III); (c) an -NR connected to the imidazolidinone ring was anticipated to structurally position Pn' into Sn' subsites; (d) The sequence of HNE is moderately similar to that of PR3 (57% identity) [20]. The comparison of substrate specificity of HNE and PR3 is shown in Figure 2.3 [36]. The S1 pocket

of HNE is hemispherical and hydrophobic [26] which prefers small residues like methyl, isobutyl, hydroxymethyl and mercaptomethyl, as well as benzyl group [28, 37]. And the S1 pocket of PR3 is smaller than that of HNE due to the replacement of Val190 by Ile190. The S2 subsite of HNE explains the preference for medium-size, hydrophobic side chains. But the S2 subsite of PR3 prefers a negatively charged P2. The S1' subsite of HNE is the main determinant of a favorable S'-P' interaction [38] which is relatively hydrophobic lining with Cys42-Cys58 and Phe41 [27]. S1'-S3' in PR3 are smaller and more polar than that of HNE. A preference of a negatively charged and more polar side-chain at P2' in PR3 would improve its interaction with the PR3 S2' subsite. These differences in substrate specificities between HNE and PR3 which depend greatly on S'-P' interactions can be exploited to design potent and selective inhibitors of HNE and PR3.

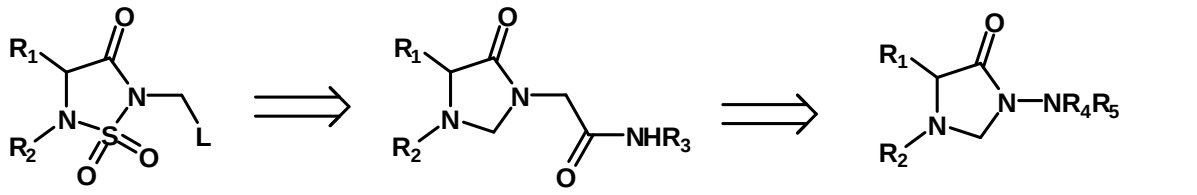

(II)
(Mechanism-based irreversible inhibitors)

(III)
(Reversible competitive inhibitors)

(I)
(Reversible competitive inhibitors of HNE and/or PR3)

Figure 2.2 Inhibitor / library design rationale

2.2 Research Goals

Based on the forgoing discussion, the goals of the research described in this thesis were:

a) Design and synthesis of potent and selective reversible inhibitors of human neutrophil elastase and proteinase 3 based on the N-amino-4-imidazolidinone scaffold;

b) *In vitro* biochemical studies to determine the potency and selectivity of the inhibitors.

CHAPTER 3

EXPERIMENTAL

3.1 Synthesis

A series of compounds **7-26** were synthesized as shown in Scheme 3.1.

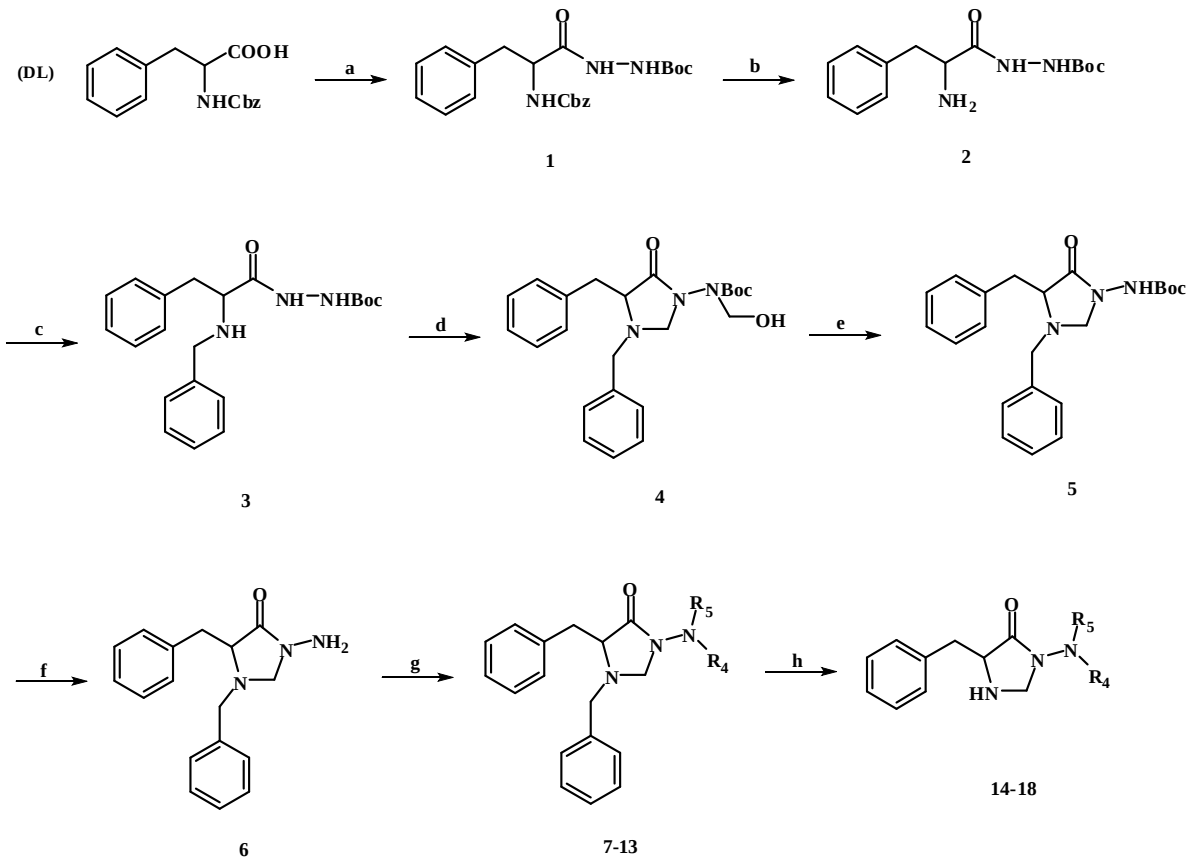

[a]IBCF/NMM/THF then t-butyl carbazate; [b]H_2/Pd/C; [c]PhCHO/$NaBH(OAc)_3$/HOAc; [d]HCHO; [e]NaOH/1,4-dioxane/H_2O; [f]silica gel/microwave; [g]$R_4N{=}C{=}O$ or R_4COOH or $(R_4CO)_2O$ or R_4SO_2Cl or protected amino acid; [h]H_2/Pd-C

Scheme 3.1 Synthesis of inhibitors. The compounds with R_1=isobutyl were synthesized using a similar procedure as that with R_1=benzyl.

3.1.1 General

The ^{1}H spectra were recorded on a Varian XL-300 or XL-400 NMR spectrometer. A Hewlett-Packard diode array UV/VIS spectrophotometer was used in the *in vitro* evaluation of the inhibitors. Human neutrophil elastase, proteinase 3 and Boc-Ala-Ala-Nva thiobenzyl ester were purchased from Elastin Products Company, Owensville, MO. Methoxysuccinyl Ala-Ala-Pro-Val p-nitroanilide and 5,5'-dithio-bis (2-nitrobenzoic acid) were purchased from Sigma Chemicals, St. Louis, MO. Melting points were determined on a Mel-Temp apparatus and are uncorrected. Reagents and solvents were purchased from various chemical suppliers (Aldrich, Acros Organics, TCI American, and Bachem). Silica gel (230-450 mesh) used for flash chromatography was purchased from Sorbent Technologies (Atlanta, GA). Thin layer chromatography was performed using Analtech silica gel plates and the TLC plates were visualized using iodine and/or UV light.

3.1.2 Representative Syntheses

*Compound **1***: A solution of Z-DL-Phe-OH (71.84 g, 240 mmol) in dry THF (200 mL) cooled in an ice-bath was treated with isobutyl chloroformate (32.78g, 31.12 mL, 240 mmol), followed with N-methylmorpholine (24.28g, 26.38 mL, 240 mmol). The resulting mixture was stirred for 5 min, and tert-butyl carbazate (31.60 g, 240 mmol) was added. The ice-bath was

removed and the reaction mixture was stirred for 7 h at room temperature. The solvent was removed and methylene chloride (200mL) was added. The resulting solution was washed with 5% aqueous HCl (70mL), 5% aqueous $NaHCO_3$ (3×70 mL) and brine (3×70 mL). The organic phase was dried over anhydrous Na_2SO_4 and the solvent was removed to yield the product (97.25g, 98%) as a white solid.

*Compound **2***: A solution of compound **1** (47.79g, 116 mmol) in methanol (250 mL) was treated with 10% palladium on carbon (7.89 g). The reaction mixture was stirred at room temperature under hydrogen (low pressure) for 3 h. The catalyst was filtered off, rinsed and the solvent was evaporated, leaving a crude product which was purified by recrystallization (ethyl acetate/hexanes) to yield the product (26.53g, 82%) as a white solid.

*Compound **3***: A solution of compound **2** (23.40 g, 83.8 mmol) and benzaldehyde (10.68 g, 100.6 mmol) in dry 1,2-dichloroethane (150 mL) was treated with glacial acetic acid (7.05 g, 117.3 mmol), followed by sodium triacetoxyborohydride (25.56 g, 117.3 mmol). The reaction mixture was stirred for 4 h at room temperature and then neutralized via the dropwise addition of cold 10% aqueous NaOH solution to pH 9-10 while stirring. The organic phase was separated and the aqueous phase was extracted with ethyl acetate (3×150 mL). The combined organic phase was dried over anhydrous Na_2SO_4 and the solvent was removed. The crude product was

purified by flash chromatography (silica gel/hexane/ethyl acetate) to yield a pure product (14.04g, 45%) as colorless oil.

*Compound **4***: A mixture of compound **3** (11.20 g, 30.31 mmol) and 37% aqueous formaldehyde (50 mL) was refluxed for 4 h. The reaction mixture was cooled to room temperature. Water (50 mL) was added, and the solution was extracted with CH_2Cl_2 (3×70 mL). The organic phase was dried over anhydrous Na_2SO_4 and the solvent was removed. The crude product was purified by flash chromatography (silica gel/hexane/ethyl acetate) to yield a pure product (6.48g, 52%) as colorless oil.

*Compound **5***: Compound **4** (12.47 g, 30.31 mmol) in 1, 4-dioxane (50 mL) was treated with a solution of KOH (29.68 g, 530 mmol) in H_2O (53 mL). The reaction mixture was stirred at room temperature for 1 h. The solvent was removed on a rotary evaporator and the resulting residue was extracted with ethyl acetate (3×70 mL). The organic phase was dried over anhydrous Na_2SO_4 and the solvent was removed. The crude product was purified by flash chromatography (silica gel/hexane/ethyl acetate) to yield a pure product (7.51g, 65%) as colorless oil.

*Compound **6***: Compound **5** (10.53 g, 27.60 mmol) was dissolved in CH_2Cl_2 (300 mL) and silica gel (0.032-0.063 mm) (140 g) was added. The solvent was taken off on a rotary evaporator and the powdered solid was irradiated in a microwave oven in an open crystallizing dish for 10

min at watts. The solid was thoroughly washed with methanol and the solvent was removed. The crude product was purified by flash chromatography (silica gel/hexane/ethyl acetate) to yield a pure product (2.33g, 30%) as colorless oil.

*Compound **7***: Compound **6** (0.56 g, 2 mmol) in dry CH_2Cl_2 (3 mL) was cooled to 0 ^oC and was then treated with triethylamine (0.33 mL, 2.4 mmol) and ethyl isocyanatoacetate (0.26 g, 0.23 mL, 2 mmol). The reaction mixture was stirred overnight at room temperature. The mixture was treated with ethyl acetate (40 mL) and then was washed successively with 5% aqueous HCl (10 mL), 5% aqueous $NaHCO_3$ (10 mL) and brine (10 mL). The organic phase was dried over anhydrous Na_2SO_4 and the solvent was removed. The crude product was purified by flash chromatography (silica gel/hexane/ethyl acetate) to yield a pure product (0.15g, 18%) as colorless oil.

*Compound **8:*** Prepared from compound **6** and phenethyl isocyanate using the similar procedure as that of compound **7** to give a pure product (72% yield) as a colorless oil.

*Compound **9***: Compound **6** (0.56 g, 2 mmol) in dry CH_2Cl_2 (10 mL) was added succinic anhydride (0.20 g, 2 mmol). The reaction mixture was stirred overnight at room temperature. The solvent was removed on a rotary evaporator and the crude was washed with 20 mL diethyl ether to give a pure product (0.54 g, 71%) as a white solid.

*Compound **10***: 1-benzyl-5-oxopyrrolidine-3-carboxylic acid (0.44 g, 2 mmol) dissolved in 20 mL DMF was treated with 1-(3-dimethylaminopropyl)-3-ethylcarbodiimide hydrochloride (0.46 g, 2.4 mmol). After the solution was stirred for 20 min, compound **6** (0.56 g, 2 mmol) was added. The resulting mixture was stirred at room temperature overnight. The solvent was removed under vacuum with an oil pump. The residue was treated with CH_2Cl_2 (70 mL) and then was washed sequentially with 5% aqueous HCl (3×20 mL), 5% aqueous $NaHCO_3$ (3×20 mL) and brine (3×20 mL). The organic phase was dried over anhydrous Na_2SO_4 and the solvent was removed. The crude product was purified by flash chromatography (silica gel/hexane/ethyl acetate) to yield a pure product (0.28g, 29%) as colorless oil.

*Compound **11:*** Prepared from compound **6** and 1-(4-fluorobenzyl)-5-oxopyrrolidine-3-carboxylic acid using the similar procedure as that of compound **10** to give a pure product (34% yield) as colorless oil.

*Compound **12:*** Prepared from compound **6** and 1-(furan-2-ylmethyl)-5-oxopyrrolidine-3-carboxylic acid using the similar procedure as that of compound **10** to give a pure product (40% yield) as colorless oil.

*Compound **13:*** Prepared from compound **6** and phthalic anhydride using the similar procedure as that of compound **9** to give a pure product (94% yield) as a white solid.

*Compound **14***: A solution of compound **8** (0.50 g, 1.2 mmol) in dry methanol (50 mL) was treated with palladium on carbon (0.35 g) under hydrogen gas. The reaction mixture was stirred for 1 h at room temperature. The catalyst was filtered off. The solvent was removed on a rotary evaporator. The crude was washed with diethyl ether (2×5 mL) to yield a pure product (0.23 g, 59%) as a white solid.

*Compound **15:*** Prepared from compound **9** using the similar procedure as that of compound **14** to give a pure product (89% yield) as a light yellow oil.

*Compound **16:*** Prepared from compound **10** using the similar procedure as that of compound **14** to give a pure product (65% yield) as colorless oil.

*Compound **17:*** Prepared from compound **11** using the similar procedure as that of compound **14** to give a pure product (71% yield) as colorless oil.

*Compound **18:*** Prepared from compound **13** using the similar procedure as that of compound **14** to give a pure product (81% yield) as a light yellow solid.

Compounds ***18*** – ***26*** were synthesized using similar procedures as those used with benzyl group.

The substituted 5-oxopyrrolidine-3-carboxylic acids were synthesized using the methods shown in Scheme 3.2.

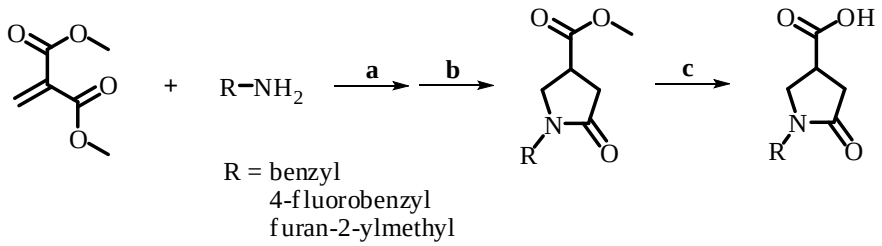

[a]methanol/RT./overnight; [b]Reflux; [c]10% aqueous KOH

Scheme 3.2 Synthesis of substituted 5-oxopyrrolidine-3-carboxylic acids

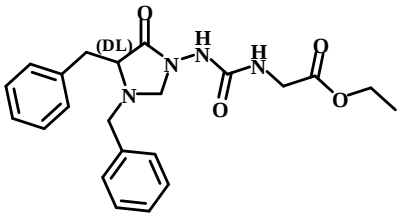

7

$C_{22}H_{26}N_4O_4$ MW: 410.47

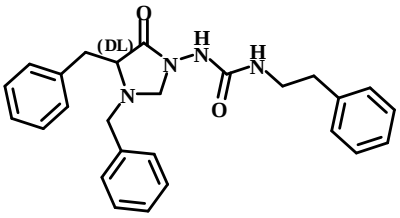

8

$C_{26}H_{28}N_4O_2$ MW: 428.53

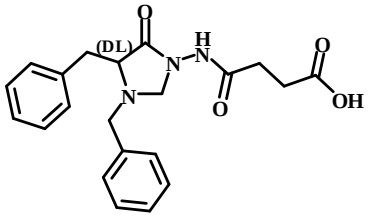

9

$C_{21}H_{23}N_3O_4$ MW: 381.43

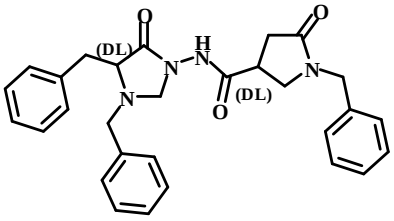

10

$C_{29}H_{30}N_4O_3$ MW: 482.57

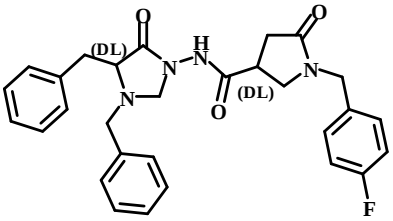

11

$C_{29}H_{29}FN_4O_3$ MW: 500.56

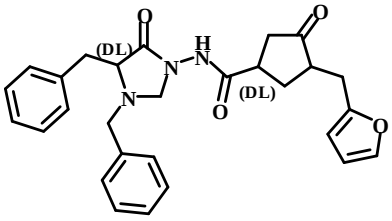

12

$C_{28}H_{29}N_3O_4$ MW: 471.55

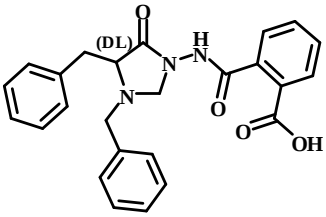

13

$C_{25}H_{23}N_3O_4$ MW: 410.47

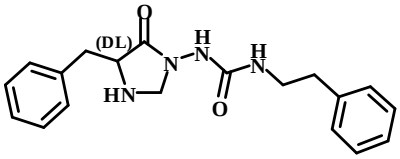

14

$C_{19}H_{22}N_4O_2$ MW: 338.40

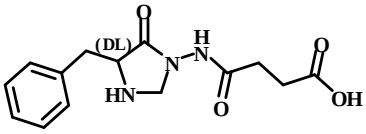

15

$C_{14}H_{17}N_3O_4$ MW: 291.30

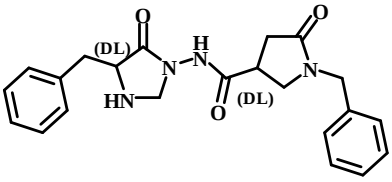

16

$C_{22}H_{24}N_4O_3$ MW: 392.45

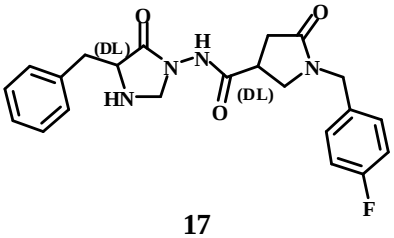

17

$C_{22}H_{23}FN_4O_3$ MW: 410.44

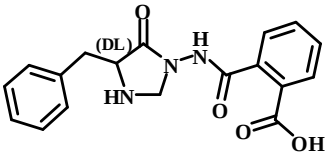

18

$C_{18}H_{17}N_3O_4$ MW: 339.35

Figure 3.1 Structures of N-amino-4-imidazolidinone derivatives **7**-**26**

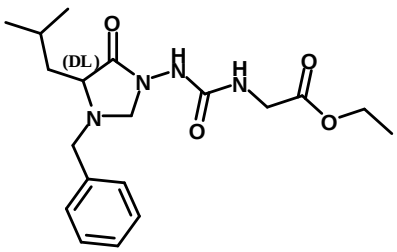

19

$C_{19}H_{28}N_4O_4$ MW: 376.45

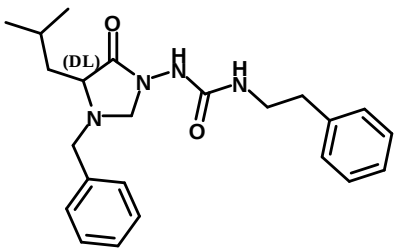

20

$C_{23}H_{30}N_4O_2$ MW: 394.51

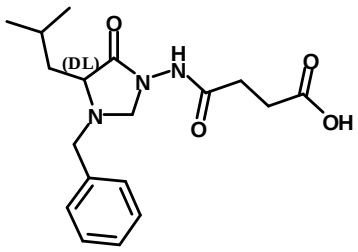

21

$C_{18}H_{25}N_3O_4$ MW: 347.41

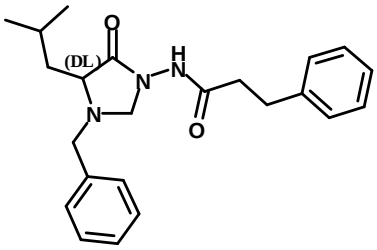

22

$C_{23}H_{29}N_3O_2$ MW: 379.50

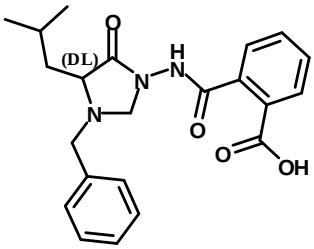

23

$C_{22}H_{25}N_3O_4$ MW: 395.45

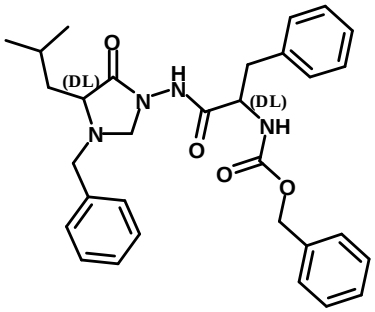

24

$C_{31}H_{36}N_4O_4$ MW: 528.64

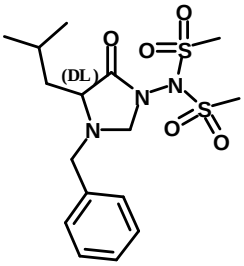

25

$C_{16}H_{25}N_3O_5S_2$ MW: 403.52

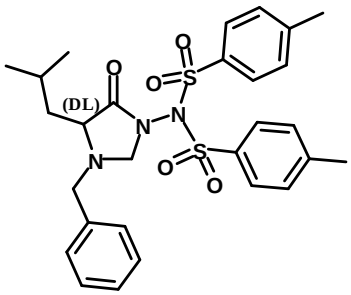

26

$C_{28}H_{33}N_3O_5S_2$ MW: 555.71

Figure 3.1 Structures of N-amino-4-imidazolidinone derivatives **7**-**26** (continued)

TABLE 3.1

PHYSICAL PROPERTIES AND ^{1}H NMR SPECTRA DATA OF COMPOUNDS **1-26**

Compound	Formula & MW (g/mol)	MP (^{o}C)	^{1}H NMR Data (δ ppm)
1	$C_{22}H_{27}N_3O_5$ MW: 413.47	120.0-121.5	1.45(s, 9H), 3.00-3.20(m, 2H), 4.41-4.52(m, 1H), 5.05(s, 2H), 5.22-5.30(d, 1H), 6.38(s, 1H), 7.08-7.38(m, 10H)
2	$C_{14}H_{21}N_3O_3$ MW: 279.33	115.0-116.0	1.48(s, 9H), 2.68-2.76(m, 1H), 3.28-3.36(m, 1H), 3.70-3.75(m, 1H), 6.45(s, 1H), 7.20-7.36(m, 5H)
3	$C_{21}H_{27}N_3O_3$ MW: 369.46	oil	1.45(s, 9H), 2.74-2.82(m, 1H), 3.19-3.24(m, 1H), 3.46-3.54(m, 1H), 3.54-3.58(d, 1H), 3.78-3.52(d, 1H), 6.82(s, 1H), 7.08-7.32(m, 10H)
4	$C_{23}H_{29}N_3O_4$ MW: 411.49	oil	1.42(s, 9H), 2.98-3.02(m, 1H), 3.08-3.15(m, 1H), 3.45-3.60(m, 2H), 3.80-3.85(d, 1H), 4.05 (s, 2H), 4.70-4.82(m, 2H), 7.05-7.50(m, 10H)
5	$C_{22}H_{27}N_3O_3$ MW: 381.47	oil	1.42(s, 9H), 2.95-3.08(m, 1H), 3.12-3.22(m, 1H), 3.44-3.50(d, 1H), 3.54-3.58(s, 1H), 3.78-3.86(d, 1H), 3.96(s, 1H), 4.02-4.12 (m, 1H), 6.30-6.42(s, 1H), 7.10-7.22(m, 10H)
6	$C_{17}H_{19}N_3O$ MW: 281.35	oil	2.85-3.02(m, 1H), 3.05-3.18(m, 1H), 3.38-3.46(d, 1H), 3.46-3.56(m, 1H), 3.72-3.84(m, 2H), 3.95-4.04(d, 1H), 7.08-7.18(m, 10H)
7	$C_{22}H_{26}N_4O_4$ MW: 410.47	oil	1.20-1.28(t, 3H), 2.92-3.15(m, 2H), 3.48-3.55(d, 1H), 3.55-3.61(m, 1H), 3.75-3.92(m, 3H), 4.00-4.19(m, 4H), 5.80(s, 1H), 7.15-7.28(m, 10H)
8	$C_{26}H_{28}N_4O_2$ MW: 428.53	oil	2.56-2.79(m, 2H), 2.91-3.12(m, 2H), 3.14-3.44(m, 2H), 3.44-3.54(d, 1H), 3.51-3.63(m, 1H), 3.80-4.00(m, 3H), 4.64-4.78(t, 1H), 6.64-6.76(s, 1H), 7.00-7.44(m, 15H)
9	$C_{21}H_{23}N_3O_4$ MW: 381.43	131.5-133.0	2.39-2.59(m, 2H), 2.64-2.74(m, 2H), 2.91-3.19(m, 2H), 3.49-3.58(d, 1H), 3.56-3.64(m, 1H), 3.73-3.82(d, 1H), 4.04-4.23(t, 2H), 7.12-7.36(m, 10H), 8.33-8.46(s, 1H)
10	$C_{29}H_{30}N_4O_3$ MW: 482.57	oil	2.50-2.80(m, 2H), 2.86-2.98(m, 1H), 3.00-3.17(m, 2H), 3.28-3.49(m, 3H), 3.48-3.56(m, 1H), 3.71-3.86(m, 1H), 3.93-4.02(t, 1H), 4.02-4.11(m, 1H), 4.30-4.42(t, 2H), 7.05-7.40(m, 15H), 9.16-9.22(d, 1H)

TABLE 3.1 (continued)

Compound	Formula	MP (^{o}C)	1H NMR Data (δ ppm)
11	$C_{29}H_{29}FN_4O_3$ MW: 500.56	oil	2.54-2.83(m, 2H), 2.91-3.18(m, 3H), 3.30-3.51(m, 3H), 3.51-3.62(m, 1H), 3.78-3.90(t, 1H), 3.97-4.12(m, 2H), 4.27-4.51(m, 2H), 6.94-7.08(m, 2H), 7.12-7.40(m, 12H), 7.66-7.80(d, 1H)
12	$C_{28}H_{29}N_3O_4$ MW: 471.55	oil	2.50-2.75(m, 2H), 2.90-3.01(m, 1H), 3.01-3.17(m, 2H), 3.37-3.63(m, 4H), 3.76-3.90(m, 1H), 4.00-4.15(m, 2H), 4.28-4.53(m, 2H), 6.20-6.30(m, 2H), 7.07-7.42(m, 11H), 8.67-8.82(d, 1H)
13	$C_{25}H_{23}N_3O_4$ MW: 410.47	132.0-134.0	2.91-3.17(m, 2H), 3.64-3.79(m, 2H), 3.79-3.89(m, 1H), 4.17-4.26(d, 1H), 4.35-4.45(d, 1H), 7.04-7.67(m, 10H), 7.75-8.08(m, 4H), 9.22(s, 1H)
14	$C_{19}H_{22}N_4O_2$ MW: 338.40	130.0-131.0	2.69-2.85(m, 2H), 2.92-3.14(m, 2H), 3.33-3.43(m, 2H), 3.70-3.82(m, 1H), 4.04-4.15(t, 1H), 4.26-4.37(m, 1H), 4.98-5.13(t, 1H), 6.97-7.11(s, 1H), 7.11-7.38(m, 10H)
15	$C_{14}H_{17}N_3O_4$ MW: 291.30	oil	2.43-2.73(m, 4H), 3.09-3.26(m, 1H), 3.30-3.47(m, 1H), 4.23-4.38(m, 1H), 4.51-4.69(m, 2H), 7.16-7.46(m, 5H)
16	$C_{22}H_{24}N_4O_3$ MW: 392.45	oil	2.57-2.84(m, 2H), 2.85-2.98(m, 1H), 2.98-3.23(m, 2H), 3.30-3.58(m, 3H), 3.68-3.78(m, 1H), 4.20-4.28(m, 1H), 4.34-4.41(m, 1H), 4.44-4.56(m, 1H), 7.05-7.42(m, 10H), 8.68-8.86(d, 1H)
17	$C_{22}H_{23}FN_4O_3$ MW: 410.44	oil	2.63-2.82(m, 2H), 2.90-3.04(m, 1H), 3.04-3.21(m, 23H), 3.34-3.57(m, 2H), 3.73-3.81(m, 1H), 4.21-4.34(m, 1H), 4.34-4.53(m, 2H), 6.93-7.07(t, 2H), 7.10-7.38(m, 7H), 8.07-8.25(d, 1H)
18	$C_{18}H_{17}N_3O_4$ MW: 339.35	123.5-125.0	2.66-2.80(m, 1H), 2.92-3.06(m, 1H), 3.15(s, 1H), 3.51-3.63(m, 1H), 4.00-4.16(m, 1H), 4.22-4.34(m, 1H), 7.12-7.40(m, 5H), 7.42-7.74(m, 4H), 7.07(s, 1H), 10.43(s, 1H)
19	$C_{19}H_{28}N_4O_4$ MW: 376.45	114.0-115.5	0.68-0.90(m, 6H), 1.10-1.24(t, 3H), 1.42-1.58(m, 2H), 1.78-1.93(m, 1H), 3.17-3.26(m, 1H), 3.57-3.66(d, 1H), 3.80-3.95(m, 3H), 3.97-4.14(m, 3H), 4.22-4.30(d, 1H), 6.24-6.36(t, 1H), 7.12-7.36(m, 5H), 8.05(s, 1H)

TABLE 3.1 (continued)

Compound	Formula	MP (°C)	1H NMR Data (δ ppm)
20	$C_{23}H_{30}N_4O_2$ MW: 394.51	oil	0.75-0.98(m, 6H), 1.46-1.64(m, 2H), 1.84-1.98(m, 1H), 2.67-2.82(t, 2H), 3.19-3.28(m, 1H), 3.30-3.45(m, 2H), 3.57-3.67(d, 1H), 3.90-4.00(d, 1H), 4.00-4.07(d, 1H), 4.23-4.51(d, 1H), 5.52-5.63(t, 1H), 7.08-7.42(m, 10H), 7.72(s, 1H)
21	$C_{18}H_{25}N_3O_4$ MW: 347.41	oil	0.70-0.82(m, 3H), 0.82-0.95(m, 3H), 1.47-1.63(m, 2H), 1.78-1.95(m, 1H), 2.40-2.58(t, 2H), 2.58-2.74(m, 2H), 3.23-3.33(m, 1H), 3.64-3.74(d, 1H), 3.90-3.98(d, 1H), 4.05-4.13(d, 1H), 4.28-4.35(d, 1H), 7.16-7.37(m, 5H), 9.06(s, 1H)
22	$C_{23}H_{29}N_3O_2$ MW: 379.50	102.0-103.5	0.74-0.97(m, 6H), 1.47-1.67(m, 2H), 1.84-1.99(m, 1H), 2.42-2.58(t, 2H), 2.84-2.98(m, 2H), 3.23-3.31(m, 1H), 3.62-3.70(d, 1H), 3.89-3.98(d, 1H), 3.98-4.06(d, 1H), 4.17-4.24(d, 1H), 7.04-7.41(m, 10H), 9.17(s, 1H)
23	$C_{22}H_{25}N_3O_4$ MW: 395.45	105.5-107.0	0.78-0.90(d, 3H), 0.95-1.07(d, 3H), 1.60-1.85(m, 2H), 1.92-2.08(m, 1H), 3.38-3.47(m, 1H), 3.86-3.95(d, 1H), 4.04-4.12(d, 1H), 4.17-4.23(d, 1H), 4.52-4.59(d, 1H), 7.20-7.48(m, 5H), 7.71-7.96(m, 4H)
24	$C_{31}H_{36}N_4O_4$ MW: 528.64	oil	0.73-0.85(m, 3H), 0.85-0.98(m, 3H), 1.47-1.66(m, 2H), 1.84-1.96(m, 1H), 2.92-3.17(m, 2H), 3.20-3.28(m, 1H), 3.57-3.68(m, 1H), 3.78-3.86(m, 1H), 3.86-3.99(m, 2H), 3.99-4.08(m, 1H), 4.85-5.06(m, 2H), 7.05-7.40(m, 10H), 8.64-8.80(d, 1H)
25	$C_{16}H_{25}N_3O_5S_2$ MW: 403.52	88.0-89.5	0.77-0.88(d, 3H), 0.88-1.03(d, 3H), 1.48-1.73(m, 2H), 1.83-2.03(m, 1H), 3.24-3.35(m, 1H), 3.35-3.50(d, 6H), 3.70-3.80(d, 1H), 3.88-3.97(d, 1H), 4.07-4.14(d, 1H), 4.45-4.53(d, 1H), 7.23-7.47(m, 5H)
26	$C_{28}H_{33}N_3O_5S_2$ MW: 555.71	83.0-85.0	0.73-0.84(d, 3H), 0.84-0.95(d, 3H), 1.34-1.71(m, 2H), 1.82-2.02(m, 1H), 2.42(s, 6H), 3.12-3.22(m, 1H), 3.67-3.77(d, 1H), 3.84-3.93(d, 1H), 4.13-4.18(d, 1H), 4.44-4.56(d, 1H), 7.20-7.45(m, 9H), 7.70-7.92(m, 4H)

3.2 Screening Method

3.2.1 Screening Procedure / Human Neutrophil Elastase

In a typical inhibition experiment, 10 µL of 7.0 µM HNE was incubated with 10 µL of 3.5 mM solution of inhibitor in DMSO ([inhibitor]/[enzyme]=500), 970 µL 0.1 M HEPES/0.5 M NaCl buffer, pH 7.25, at 25 ^{o}C. After 30 min, 10 µL of 70 mM methoxysuccinyl-Ala-Ala-Pro-Val *p*-nitroanilide was added and the amount of active enzyme was determined by monitoring the release of *p*-nitroaniline at 410 nm for 2 minutes. A control (hydrolysis) containing 970 µL 0.1 M HEPES/0.5 M NaCl buffer, pH 7.25, 10 µL of 7.0 µM HNE, 10 µL DMSO, and 10 µL of 70 mM methoxysuccinyl-Ala-Ala-Pro-Val *p*-nitroanilide was run under the same conditions. The degree of inhibition was expressed as % inhibitor = $[1 - (/v_0)] \times 100$ (v_0 is the enzymatic catalysis velocity of the control while v is that of inhibition experiment.), and is the average of duplicate or triplicate determinations.

3.2.2 Screening Procedure / Proteinase 3

Ten microliters of a 1.73 mM inhibitor solution in DMSO ([inhibitor]/[enzyme]=500) and 20 µL of 12.98 mM Boc-Ala-Ala-Nva-SBzl in DMSO were added to a cuvette containing 940 µL 0.1 M HEPES/0.5 M NaCl buffer, pH 7.25. After the solution was well mixed, 20 µL of 32 mM 5,5'-dithio-bis(2-nitrobenzioc acid) in DMSO and 10 µL of 3.45 µM solution of proteinase

3 in 0.1 M phosphate/0.25 M NaCl buffer, pH 6.50, were added and the change in absorbance was monitored at 410 nm for 2 minutes. A control (hydrolysis) containing 940 µL 0.1 M HEPES/0.5 M NaCl, pH 7.25, 10 µL 3.40 µM solution of proteinase 3, 20 µL DMSO, 20 µL of 16 mM 5,5'-dithio-bis(2-nitrobenzioc acid) in DMSO, and 20 µL of 6.49 mM Boc-Ala-Ala-Nva-SBzl in DMSO was also run under the same condition. Determinations were performed in duplicate or triplicate and inhibition of inhibitors was calculated as described for HNE.

3.3 Dixon Plot

Add 970 µL 0.1 M HEPES/0.5 M NaCl buffer, pH 7.25, in 6 cuvettes. 0, 2, 4, 6, 8, 10 µL of 5 mM solution of inhibitor in DMSO ([inhibitor]/[enzyme]=250), and 10, 8, 6, 4, 2, 0 µL DMSO were added to each cuvette in sequential order for final inhibitor concentrations of 0 to 50 µL. Then 10 µL of 7.0 µM HNE, and 10 µL of 35 mM methoxysuccinyl-Ala-Ala-Pro-Val *p*-nitroanilide were added. The amount of active enzyme was determined by monitoring the release of *p*-nitroaniline at 410 nm for 2 minutes. For the second assay, 70 mM methoxysuccinyl-Ala-Ala-Pro-Val *p*-nitroanilide was added.

3.4 Computational Method

Molecular docking simulation was performed using AUTODOCK4.0 program [39]. The structures of inhibitors **24** and **17** were constructed in SYBYL8.0 [40] and were structrally

optimized to default convergence thresholds using the Tripos Force field [41] and Gasteiger-Marsili partial actomic charges [42]. The receptor models were prepared for HLE and PR3 using the 1PPF [25] and 1FUJ [28] crystal structures respectively. The reversible inhibitor was removed from crystal structure 1PPF using AUTODOCK4.0 and all water molecules were stripped off from both structures. These structures were electrostatically represented with Gasteiger-Marsili charges.

CHAPTER 4

RESULTS AND DISCUSSION

4.1 Synthesis of Inhibitors

Inhibitors **7**-**26** were synthesized as shown in Scheme 3.1 to probe the Sn and Sn' subsites of HNE and PR3. (DL) Benzyloxycarbonyl-protected phenylalanine or leucine *t*-butyl hydrazinecarboxylate was produced by treating Z-DL-phenylalanine with isobutyl chloroformate, N-methylmorpholine and *tert*-butyl carbazate. After N-terminal deprotection, reductive amination was carried out using an appropriate aldehyde in the presence of sodium borohydride to yield alkylated product **4**. This was reacted with aqueous formaldehyde to form the heterocyclic ring. The cyclization reaction was successful; however, the product underwent further N-hydroxymethylation to give compound **4**. The hydroxymethyl group was removed by treatment with dilute base. Removal of the Boc group using silica gel and microwave irradiation yielded compound **6** in low yield. This step was successful, however the yields were erratic. Further elaboration gave a series of highly functionalized N-amino-4-imidazolidinones (listed In Figure 3.1). In our previous studies, inhibitors with an isobutyl or benzyl group as P1 showed great preference with S1 subsite of HNE. Modification of P2 and Pn' recognition elements yielded a series of compounds that were anticipated to dock to the active site of HNE and PR3.

4.2 Biochemical results

A series of potential inhibitors of human neutrophil elastase and proteinase 3 based on the N-amino-4-imidazolidinone scaffold were designed and synthesized using combinational chemistry. Different P1, P2 and Pn' residues were used to probe the Sn' subsites of HNE and PR3. These compounds were then screened against HNE and PR3.

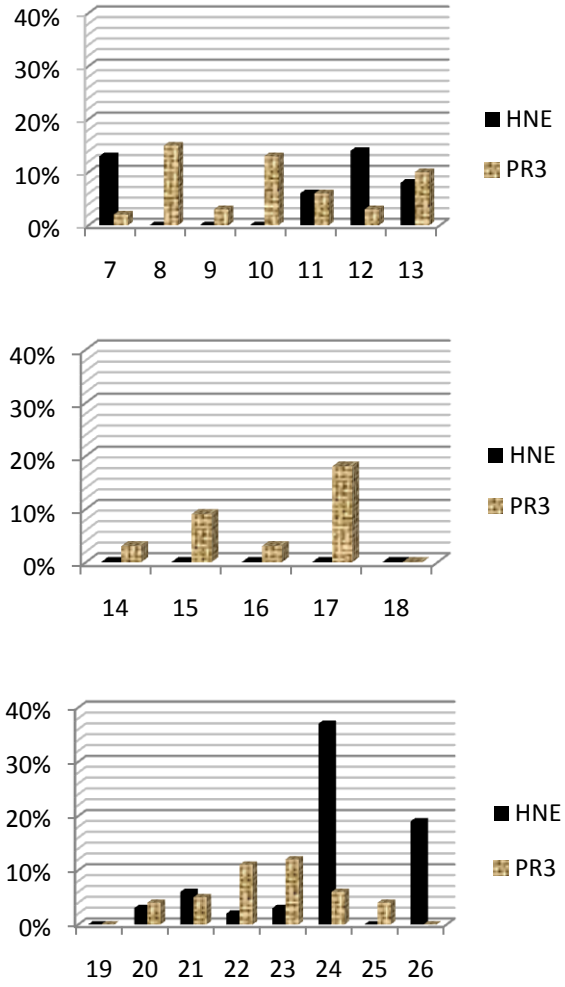

Figure 4.1 Screening results of inhibitors **7-26** against HNE and PR3

Although the compounds show weak inhibition against PR3 (Figure 3.2), inhibitor **17** has been found to inhibit PR3 better than other compounds (18% inhibition), and has very low inhibition towards HNE. Inhibitor **24** had the highest percent inhibition (37%) against HNE, but only 6% percent inhibition against PR3. It was demonstrated to be a good competitive reversible inhibitor of HNE by Dixon plot with a K_I of 7.34 μM (Figure 4.1). The results suggest that HNE and PR3 show different preference for (I) depending on the nature of the P1, P2 and Pn' residues.

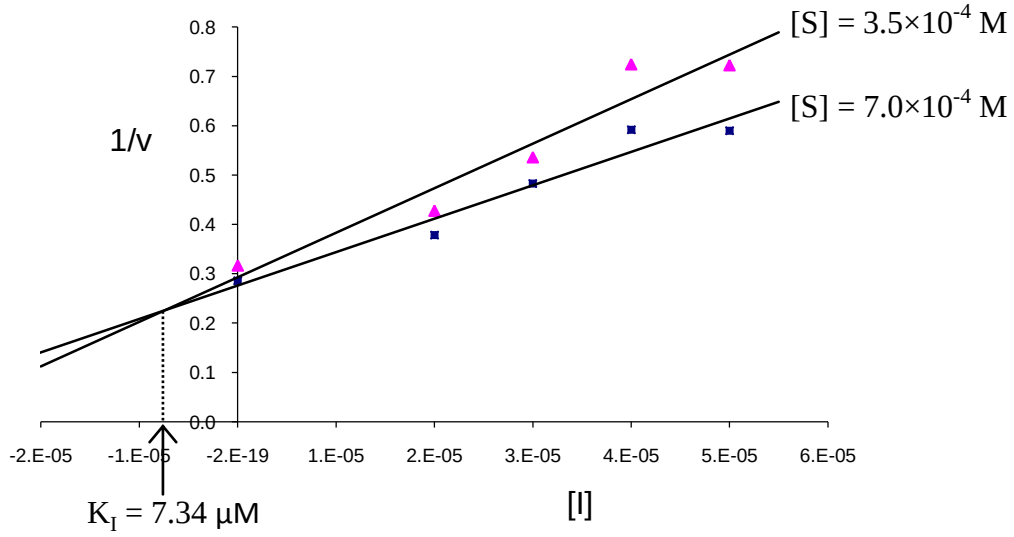

Figure 4.2 Dixon plot of inhibitor **24** against HNE and the determination of K_I

4.3 Molecular Docking Simulation

From molecular docking simulation, the best binding affinity of compound **24** towards HNE is the (L, D) isomer (Figure 4.2A). Its isobutyl group binds to a hydrophobic S1 pocket defined by Val190 and Phe192. One of the carbonyl oxygen appears to accept H-bonds from NH of the backbone Phe192. The three phenyl rings are well positioned to interact with three shallow hydrophobic pockets. When this isomer was docked into the PR3 active site (Figure 4.2C), it appears that the phenyl ring binds to the S1 pocket and the rest of hydrophobic substitutions occupy the shallow S pockets. It was found to be less potent than inhibitor **17**.

Figure 4.2D is the docking model of the (D, L) isomer of **17** with PR3. The benzyl ring binds to the S1 pocket of PR3, defined by Ile190 and Phe192. The N-H of the secondary amine donates H-bond to the carbonyl group of the backbone Ser214. The p-fluorobenzyl group occupies the S' pockets. Figure 4.2B shows the (D, L) isomer of compound **17** docked into HNE active site. The benzyl group occupies the S1 pocket and the p-fluorobenzyl group is projecting the S' pockets. It has weak inhibition against HNE because of lack of H-bonding and less hydrophobic interactions.

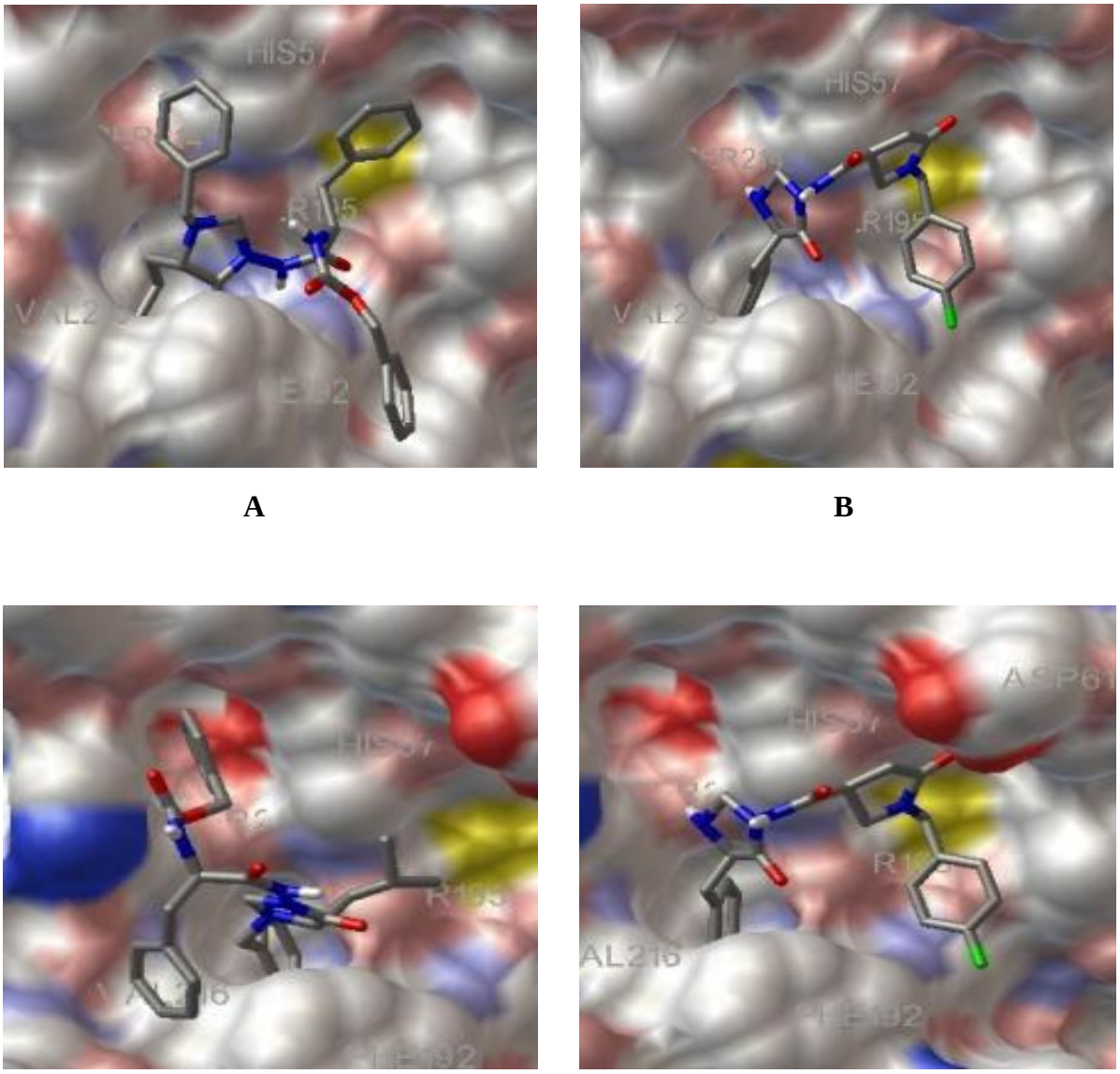

A **B**

C **D**

Figure 4.3 The molecular docking simulation of inhibitors **17** and **24**. (A) Inhibitor **24** bound to HNE; (B) Inhibitor **17** bound to HNE; (C) Inhibitor **24** bound to PR3; (D) Inhibitor **17** bound to PR3. Ligand rendered as CPK-colored sticks. Receptor surface is represented by David-Goodsell colors.

CHAPTER 5

CONCLUSIONS

A series of libraries was constructed based on a highly-functionalized N-amino-4-imidazolidinone scaffold and then screened against human neutrophil elastase and human neutrophil proteinase 3. Compound **24** was found as a selective reversible competitive inhibitor against HNE, but not PR3; whereas compound **17** showed reversible selective inhibition against PR3 instead of HNE. Construction of a Dixon plot confirmed that compound **24** was a reversible competitive inhibitor with K_I of 7.34 μM, suggesting that compound **24** is a good "Hit" compound which can be further developed to obtain selective reversible competitive inhibitors of HNE. Molecular modeling supported the biological result and could help the "Hit-to-Lead" optimization.

REFERENCES

REFERENCES

1. Richens, J.L.; Urbanowicz, R.A.; Lunt, E.A.; Metcalf, R.; Corne, J.; Fairclough, L.; O'Shea, P. (2009) *Systems Biology Coupled with Label-free High-throughput Detection as a Novel Approach for Diagnosis of Chronic Obstructive Pulmonary Disease*, **Respiratory Research**, 10: 29

2. Barnes, P.J. (2004) *Small Airways in COPD*, **N. Engl. J. Med.**, 350: 2635-2637

3. Maclay, J.D.; Rabinovich, R.A.; MacNee, W. (2009) *Update in Chronic Obstructive Pulmonary Disease 2008*, **Am. J. Respir. Crit. Care Med.**, 179: 533-541

4. Dennis, R.J.; Maldonado, D.; Norman, S.; Baena, E.; Castano, H.; Martinez, G.; Velez, J.R. (1996) *Wood Smoke Exposure and Risk for Obstructive Airways Disease Among Women*, **Chest**, 109: 55S-56S

5. Lokke, A.; Lange, P.; Scharling, H.; Fabricius, P.; Vestbo, J. (2006) *Developing COPD: A 25 Year Follow Up Study of the General Population*, **Thorax**, 61: 935-939

6. Brown, C.; Crombie, I.; Tunstall-Pedoe, H. (1994) *Failure of Cigarette Smoking to Explain International Differences in Mortality from Chronic Obstructive Pulmonary Disease*, **J. Epidemiol Community**, 48: 134-139

7. Mannino, D.M.; Buist, A.S. (2007) *Global Burden of COPD: Risk Factors*, **Lancet**, 370: 765-773

8. Ngan, D.A.; Vickerman, S.V.; Granville, D.J.; Man, S.F.P.; Sin D.D. (2009) *The Possible Role of Granzyme B in the Pathogenesis of Chronic*, **Therapeutic Advances in Respiratory Disease**, 3: 113-129

9. Barnes, P.J.; Peter, J.; (2005) *Inflammatory Mechanisms in Chronic Obstructive Pulmonary Disease*, **Science & Medicine**, 9: 252-263

10. Olivieri, D.; Pesci, A.; Bertorelli, G. (1996) *Immunological Defenses in Airways*, **Lung Biology in Health and Disease**, 93(Environmental Impact on the Airways): 43-69

11. MacNee, W. (2006) *Oxidative Stress and Chronic Obstructive Pulmonary Disease*, **Eur. Respir. Monograph**, 11: 100-129

12. Rangasamy, T.; Misra, V.; Zhen, L.; Tankersley, C.G.; Tuder, R.M.; Biswal, S. (2009) *Cigarette Smoke-induced Emphysema in A/J Mice is Associated with Pulmonary Oxidative Stress, Apoptosis of Lung Cells, and Global Alterations in Gene Expression*, **Am. J. Physiology**, 296: L888-L900

13. Armstrong, J.; Sargent, C.; Singh, D. (2009) *Glucocorticoid Sensitivity of Lipopolysaccharide-stimulated Chronic Obstructive Pulmonary Disease Alveolar Macrophages*, **Clinical and Experimental Immunology**, 158: 74-83

14. Lucey, E.C.; Stone, P.J.; Breuer, P.G.; Christensen, P.G.; Calore, J.D.; Catanese, A.; Franzblau, C.; Snider, G.L. (1985) *Effect of Combined Human Neutrophil Cathepsin G and Elastase on Induction of Secretary Cell Metaplasia and Emphysema in Hamsters with in vitro Observations on Elastolysis by These Enzymes*, **Am. Rev. Respir. Dis.**, 132: 362-366

15. Kao, R.C.; Wehner, N.G.; Skubitz, K.M.; Gray, B.H.; Hoidal, J.R. (1988) *Proteinase 3 – A Distinct Human Polymorphonuclear Leukocyte Proteinase That Produces Emphysema in Hamsters*, **J. Clin. Invest.**, 82: 1963-1973

16. Raptis, S.Z.; Shapiro, S.D.; Simmons, P.M.; Cheng, A.M.; Pham, C.T.N. (2005) *Serine Protease Cathepsin G Regulates Adhesion-Dependent Neutrophil Effector Functions by Modulating Integrin Clustering*, **Immunity**, 22: 679-691

17. Schechter, I.; Berger, A. (1967) *On The Size of The Active Site in Proteases. I. Papain.*, **Biochem. Biophys. Res. Comm.**, 27: 157-162

18. Simpson, R.J. (2003**)** *Peptide Mapping and Sequence Analysis of Gel-Resolved Proteins*, **Cold Spring Harbor Laboratory Press, NY**

19. (a) Edwards, S. W. (1994) *Biochemistry and Physiology of the Neutrophil.* **Cambridge University Press, New York, NY**; (b) Ganz, T. (2003*) Defensins: antimicrobial peptides of innate immunity*, **Nature Rev. Immunol.**, 3: 710-720

20. Senior, R.W.; Shapiro, S.D. (1998) *COPD: Epidemiology, Pathophysiology, and Pathogenesis in Fishman's Pulmonary Diseases and Disorders*, 3rd ed., **McGrawHill: NY**, pp 659-628

21. Bugg, T. (2004) *Introduction to Enzyme and Coenzyme Chemistry*, **Black Well Publishing, UK**

22. Koshland, D. E., Jr. (1958) *The Active Site and Enzyme Action*, **Advances in Enzymology and Related Subjects of Biochemistry**, 22: 45-97

23. Copeland, R.A. (2005) *Evaluation of Enzyme Inhibitors in Drug Discovery – A Guide for Medicinal Chemists and Pharmacologists*, **John Wiley & Sons, Inc., Hoboken, New Jersey**

24. Korkmaz, B.; Moreau T.; Gauthier, F. (2008) *Neutrophil Elastase, Proteinase 3 and Cathepsin G: Physicochemical Properties, Activity and Physiopathological Functions*, **Biochimie**, 90: 227-242

25. Bode, W.; Wei, A.Z.; Huber, R.; Meyer, E.; Travis, J.; Neumann, S. (1986) *X-ray Crystal Structure of The Complex of Human Leukocyte Elastase (PMN Elastase) and The Third Domain of The Turkey Ovomucoid Inhibitor*, **EMBO J.**, 5: 2453-2458

26. Navia, M.A.; McKeever, B.M.; Springer, J.P.; Lin, T.Y.; Williams, H.R.; Gluder, E.M.; Dorn, C.P.; Hoogsteen, K. (1989) *Structure of Human Neutrophil Elastase in Complex With a Peptide Chloromethyl Ketone Inhibitor at 1.84-A Resolution*, **Proc. Natl. Acad. Sci. USA**, 86: 7-11

27. Wei, A.Z.; Mayr, I.; Bode, W. (1988) *The Refined 2.3 A Crystal Structure of Human Leukocyte Elastase In a Complex With a Valine Chloromethyl Ketone Inhibitor*, **FEBS Lett.**, 234: 367-373

28. Fujinaga M.; Chernaia M.M.; Halenbeck R.; Koths K., James M.N.G. (1996) *The Crystal Structure of PR3, a Neutrophil Serine Proteinase Antigen of Wegener's Granulomatosis Antibodies*, **J. Mol. Biol.**, 261: 267-278

29. Hajjar E.; Korkmaz B.; Gauthier F.; Brandsdal B.O.; Witko-Sarsat V.; Reuter N. (2006) *Inspection of The Binding Sites of Proteinase 3 for The Design of a Highly Specific Substrate*, **J. Med. Chem.**, 49: 1248-1260

30. Korkmaz B.; Hajjar E.; Kalupov T.; Reuter N.; Brillard-Bourdet M.; Moreau T.; Juliano L.; Gauthier F. (2007) *Influence of Charge Distribution at The Active Site Surface on The Substrate Specificity of Human Neutrophil Protease 3 and Elastase. A Kinetic and Molecular Modeling Analysis*, **J. Biol. Chem.**, 282: 1989-1997

31. Korkmaz B.; Attucci S.; Moreau T.; Godat E.; Juliano L. (2004) *Design and Use of Highly Specific Substrates of Neutrophil Elastase and Proteinase 3*, **Am. J. Respir. Cell Mol. Biol.**, 30: 801-807

32. Pauling, L. (1946) *Molecularar chitecture and biological reactions*, **Chemical & Engineering News**, 24: 1375-1377

33. Menger, F.M. (1992) *Analysis of Ground-State and Transition-State Effects in Enzyme Catalysis*, **Biochemistry**, 31: 5368-5373

34. (a) Groutas, W.C.; Kuang, R.; Venkatarama, R.; Epp, J.B.; Ruan, S.; Prakash, O. (1997) *Structure Design of a General Class of Mechanism-based Inhibitors of the Serine Proteinases Employing a Novel Amino Acid Derived Heterocyclic Scaffold*, **Biochemistry**, 36: 4739-4750 (b) Lai, Z.; Gan, X.; Wei, L.; Alliston, K.; Yu, H.; Li, Y.H.; Groutas, W.C. (2004) *Potent Inhibition of Human Leukocyte Elastase by 1,2,5-thiadiazolidin-3-one 1,1 Dioxide-based Sulfonamide Derivatives*, **Arch. Biochem. Biophys.**, 429: 191-197

35. Wei, L.; Gan, X.; Zhong, J.; Alliston, K.R.; Groutas, W.C. (2003) *Noncovalent Inhibitors of Human Leukocyte Elastase based on the 4-Imidazolidinone Scaffold*, **Bioorg. Med. Chem.**, 11: 5149-5153

36. Korkmaz, B.; Hajjar, E.; Kalupov, T.; Reuter, N.; Brillard-Bourdet, M.; Moreau, T.; Juliano, L.; Gauthier, F. (2007) *Influence of Charge Distribution at the Active Site Surface on the Substrate Specificity of Human Nertrophil Protease 3 and Elastase: A Kinetic and Molecular Modeling Analysis*, **The Journal Of Biological Chemistry**, 282: 1989–1997

37. Blow, A.M.; Barrett, A.J. (1977) *Action of Human Cathepsin G on The Oxidized B Chain of Insulin*, **Biochem. J.**, 161: 17-19

38. Stein, R.L.; Strimpler, A.M. (1987) *Catalysis by Human Leukocyte Elastase. Aminolysis of Acyl-enzyme by Amino Acid Amides and Peptides*, **Biochemistry**, 26: 2238-2242

39. AUTODOCK4.0, (2007) **The Scripps Research Institute, San Diego, CA**

40. SYBYL 8.0, (2008) **Tripos Associates, St. Louis, MO**

41. Clark, M.; Cramer, R.D., III; Van Opdenbosch, N. (1989) *Validation of the General Purpose Tripos 5.2 Force Field*, **J. Comput. Chem.**, 10: 982-1012

42. Gasteiger, J.; Marsili, M. (1978) *A New Model for Calculating Atomic Charges in Molecules*, **Tetrahedron Lett.**, 34: 3181-3184